BRAIN
ORIGINAL ARTICLE

Spatially resolved neural slowing predicts impairment and amyloid burden in Alzheimer's disease

Alex I. Wiesman,[1,2] Daniel L. Murman,[2,3] Rebecca A. Losh,[4] Mikki Schantell,[4] Nicholas J. Christopher-Hayes,[4] Hallie J. Johnson,[4] Madelyn P. Willett,[4] Sara L. Wolfson,[5] Kathryn L. Losh,[4] Craig M. Johnson,[6] Pamela E. May[2] and Tony W. Wilson[4]

An extensive electrophysiological literature has proposed a pathological 'slowing' of neuronal activity in patients on the Alzheimer's disease spectrum. Supported by numerous studies reporting increases in low-frequency and decreases in high-frequency neural oscillations, this pattern has been suggested as a stable biomarker with potential clinical utility. However, no spatially resolved metric of such slowing exists, stymieing efforts to understand its relation to proteinopathy and clinical outcomes. Further, the assumption that this slowing is occurring in spatially overlapping populations of neurons has not been empirically validated.

In the current study, we collected cross-sectional resting state measures of neuronal activity using magnetoencephalography from 38 biomarker-confirmed patients on the Alzheimer's disease spectrum and 20 cognitively normal biomarker-negative older adults. From these data, we compute and validate a new metric of spatially resolved oscillatory deviations from healthy ageing for each patient on the Alzheimer's disease spectrum.

Using this Pathological Oscillatory Slowing Index, we show that patients on the Alzheimer's disease spectrum exhibit robust neuronal slowing across a network of temporal, parietal, cerebellar and prefrontal cortices. This slowing effect is shown to be directly relevant to clinical outcomes, as oscillatory slowing in temporal and parietal cortices significantly predicted both general (i.e. Montreal Cognitive Assessment scores) and domain-specific (i.e. attention, language and processing speed) cognitive function. Further, regional amyloid-β accumulation, as measured by quantitative ^{18}F florbetapir PET, robustly predicted the magnitude of this pathological neural slowing effect, and the strength of this relationship between amyloid-β burden and neural slowing also predicted attentional impairments across patients.

These findings provide empirical support for a spatially overlapping effect of oscillatory neural slowing in biomarker-confirmed patients on the Alzheimer's disease spectrum, and link this effect to both regional proteinopathy and cognitive outcomes in a spatially resolved manner. The Pathological Oscillatory Slowing Index also represents a novel metric that is of potentially high utility across a number of clinical neuroimaging applications, as oscillatory slowing has also been extensively documented in other patient populations, most notably Parkinson's disease, with divergent spectral and spatial features.

1   Montreal Neurological Institute, McGill University, Montreal, Quebec, Canada
2   Department of Neurological Sciences, University of Nebraska Medical Center (UNMC), Omaha, NE, USA
3   Memory Disorders & Behavioral Neurology Program, UNMC, Omaha, NE, USA
4   Institute for Human Neuroscience, Boys Town National Research Hospital, Boys Town, NE, USA

5   Geriatrics Medicine Clinic, UNMC, Omaha, NE, USA
6   Department of Radiology, UNMC, Omaha, NE, USA

Correspondence to: Alex I. Wiesman, PhD
Montreal Neurological Institute, McGill University
845 Sherbrooke St W, Montreal
Quebec H3A 0G4, Canada
E-mail: alexander.wiesman@mcgill.ca

Introduction

Alzheimer's disease is a neurological disorder characterized by an initial slow aggregation of amyloid-β protein deposits across the neocortex, followed by a much more rapid pattern of hyper-phosphorylated tau accumulation. This pathological build-up of tau 'tangles' is mirrored by functional and structural neuronal degradation, which eventually leads to declines in cognition.[1–4] Importantly, tau pathology is highly predictive of eventual cognitive decline in older adults with suspected Alzheimer's disease, whereas links between amyloid-β accumulation and general or domain-specific cognitive declines are less supported.[5–8] With the increasing conceptualization of Alzheimer's disease as a progressive spectrum or continuum of pathological changes, objective continuous measures of these changes are sorely needed for both research and clinical evaluation. Among candidate measures for this purpose, functional brain activity metrics have emerged as a promising option, as these changes appear relatively early in the course of the disease.[2,9,10]

Functional neuroimaging studies in Alzheimer's disease have overwhelmingly used functional MRI and focused on Alzheimer's disease-related changes during the resting-state. This literature has generally reported that patients with Alzheimer's disease exhibit aberrant neural activity in default mode and medial temporal regions.[11–15] More generally, studies of global functional connectivity in these patients have found systematic decreases in communication between spatially disparate regions, paired with increased local interactions.[15] While these investigations have been valuable for understanding the functional neural pathology in patients with Alzheimer's disease, they have largely ignored the rapid and highly dynamic nature of neuronal information processing in the human brain. Complementing this line of research, a number of investigations have leveraged techniques with better temporal precision to study Alzheimer's disease. In particular, research using EEG and magnetoencephalography (MEG) has proven useful in understanding the temporal and spectral properties of functional neuronal pathology in these patients.

The rhythmic patterning of neural activity, termed oscillations, has been identified as a particularly useful characteristic to understand functional pathology in patients with Alzheimer's disease.[16–22] Measured in cycles per second (i.e. Hz), the speed of such oscillations provides a spectral signature of the underlying population-level neuronal activity in cognitively normal adults,[23–27] as well as functional neuronal pathology in those with various neurological disorders.[28–31] These spectrally defined patterns of neural activity appear particularly relevant to the pathophysiology of Alzheimer's disease, as they have been found to covary strongly with genetic[32,33] and pathological[34–37] hallmarks of the disease. Electrophysiological investigations of patients with Alzheimer's disease have consistently reported stronger oscillatory activity in the slower delta (1–4 Hz) and theta (4–7 Hz) frequencies, accompanied by weaker oscillations in the faster alpha (7–13 Hz) and beta (15–30 Hz) frequencies.[16,17,19–22,38–45] As such, this pattern has been termed a neuronal 'slowing' effect and is thought to bear meaningful information regarding the pathological processes at play in Alzheimer's disease.

However, limitations persist in this extensive literature. First and foremost, the few previous MEG and EEG studies that have statistically tested for a neuronal slowing effect in Alzheimer's disease have been restricted spatially[20,46,47] and/or spectrally,[47–49] limiting interpretation. Conversely, previous analyses reporting co-occurring effects of increased low-frequency and decreased high-frequency activity in Alzheimer's disease[16,17,19,34,37] have not statistically tested whether these effects represent oscillatory slowing within overlapping neuronal populations. A unified multi-spectral, spatially resolved metric representing the slowing of neural activity would be exceedingly useful in this regard. Second, no continuous metric of this slowing has been conceived that properly weights each functionally meaningful oscillatory rhythm in a way that is unbiased by the natural differences in amplitude across frequencies. While ratios of fast versus slow oscillatory amplitudes have been suggested as such a metric,[46] these ratios do not control for bias introduced by frequencies with inherently higher amplitudes, an effect which varies non-linearly across the cortex. Spectrum compensation has been used towards this goal in previous work,[37] but a normalization that does not rely on theoretical data distributions (i.e. 1/f brain activity) that are now known to be altered in numerous disease states would be preferable.[50–54]

In this study, we leverage the high temporal and spatial precision of source-reconstructed MEG to provide the first direct evidence for a spatially overlapping neural slowing effect in patients on the Alzheimer's disease spectrum. Importantly, this index was normalized to spatially and spectrally comparable estimates of neural power from a group of demographically matched cognitively normal participants, making it robust against non-uniform amplitude biases across frequencies and brain regions. Termed the pathological oscillatory slowing index (POSI; Fig. 1), this spatially resolved continuous metric was generated per each biomarker-confirmed patient on the Alzheimer's disease spectrum, and

used to test for significant regions of cortical oscillatory slowing in these patients, as well as significant relationships between neuronal slowing, cognitive outcomes and regional amyloid-β deposition. We hypothesized that significant slowing would be found in cortical regions typically associated with early declines in Alzheimer's disease, including the middle and medial temporal, inferior parietal and prefrontal cortices. In addition, we expected that oscillatory slowing in these regions would relate to worsened cognitive performance in patients on the Alzheimer's disease spectrum and would covary with the severity of regional amyloid-β burden, indicating that this effect is indeed pathological in nature.

Materials and methods

Participants

The Institutional Review Board at the University of Nebraska Medical Center reviewed and approved this investigation, and all research protocols complied with the Declaration of Helsinki. Written informed consent was obtained from each participant (and, for participants in the Alzheimer's disease spectrum group, from their spouse/child informant) following detailed description of the study. For individuals with diminished capacity to make an informed decision regarding research participation, educated assent was acquired from the participant, in addition to informed consent of their legally authorized representative. All participants completed the same experimental protocol. Exclusionary criteria for both groups included any medical illness affecting CNS function, any neurological disorder (other than Alzheimer's disease), history of head trauma, moderate or severe depression (Geriatric Depression Scale ⩾ 10) and current substance abuse.

Alzheimer's disease spectrum group

Forty-four participants were screened for recruitment into the Alzheimer's disease spectrum group after referral from a memory disorders clinic where they were being treated for amnestic complaints. Prior to being screened for this study, all such participants were determined as having either amnestic mild cognitive impairment (aMCI) or mild probable Alzheimer's disease by a fellowship-trained neurologist using standard clinical criteria.[55] In addition to one of these diagnoses, a positive biomarker (using whole-brain quantitative amyloid-β PET scans) was also required for inclusion into the final Alzheimer's disease spectrum participant sample. One participant was excluded from this group due to a major incidental finding that was likely to impact cognitive function and another disenrolled due to COVID-19-related health concerns. Four additional participants were excluded after their whole-brain amyloid-β PET scanning (see 'Florbetapir ^{18}F PET' section) indicated amyloid-β-negativity. After exclusions, 38 amyloid-β-positive participants remained for inclusion into the Alzheimer's disease spectrum group.

Healthy ageing comparison group

For comparison and normalization of the Alzheimer's disease spectrum group to an analogous group of cognitively normal older adults, 20 additional participants who reported no subjective cognitive concerns were screened for inclusion into the study. Nineteen of these participants had received a biomarker test for amyloid-β positivity within the past 5 years and were confirmed biomarker-negative, while one participant received no such test, but performed exceedingly well on all neuropsychological tests. The 19 amyloid-β-negative participants were recruited based on

their prior enrolment in an unrelated anti-amyloid clinical trial in cognitively healthy older adults; because they were discovered to be amyloid-β-negative during the screening process, they were excluded from participation. These participants did not report cognitive disturbances, which was confirmed by our own detailed neuropsychological assessments.

Demographics and domain-specific neuropsychological scores for each group, as well as comparisons between groups, can be found in Supplementary Table 1. Essential demographic factors were matched across the groups with the exception of age, such that patients on the Alzheimer's disease spectrum were younger than those in the cognitively normal group. As such, all statistical analyses were performed with age included as a nuisance covariate.

Florbetapir ^{18}F PET acquisition and analysis

Combined PET/CT data using ^{18}F-florbetapir (Amyvid™, Eli Lilly) were collected following procedures described by the Society of Nuclear Medicine and Molecular Imaging (3D acquisition; single intravenous slow-bolus < 10 ml; dose = 370 MBq; waiting period = 30–50 min; acquisition = 10 min).[56] A GE Discovery MI digital PET/CT scanner was used to acquire whole-brain quantitative images of amyloid-β uptake. More details on the PET processing pipeline can be found in the Supplementary material.

Neuropsychological testing

All participants completed a battery of neuropsychological tests, after which raw scores for each participant were converted to demographically adjusted z-scores based on published normative data.[57–60] The testing battery was developed in collaboration with a clinical neuropsychologist specializing in memory disorders. We focused on five cognitive domains impacted in patients with Alzheimer's disease: verbal memory, learning, attention and executive function, verbal function and processing speed (see the Supplementary material for details). General cognitive status was measured using the Montreal Cognitive Assessment (MoCA)[61] and the Mini-Mental State Examination.[62]

MEG recording and preprocessing

Participants were seated in a custom-made non-magnetic chair with their head positioned within the MEG sensor array, and rested with their eyes closed for 8 min. This recording duration is more than double the current recommendations for healthy participants[63] and is on the higher end of what has been used historically in MEG studies of Alzheimer's disease.[19,33–35,37,43,64–68] All recordings were conducted in a one-layer magnetically shielded room with active shielding engaged. Neuromagnetic responses were sampled continuously at 1 kHz with an acquisition bandwidth of 0.1–330 Hz using a 306-sensor Elekta/MEGIN MEG system equipped with 204 planar gradiometers and 102 magnetometers. To control for general drowsiness, we collected the resting-state data at the beginning of the visit, making it less likely that participants would be cognitively fatigued at the time of data collection. In addition, an MEG technologist continuously monitored participants during data acquisition via real-time audio-video feeds from inside the shielded room. Participants whose neural data or physical demeanour suggested that they had fallen asleep, or who reported falling asleep or excessive drowsiness, were indicated as such in our logs and asked to repeat the resting-state recording. Each MEG dataset was individually corrected for head motion and subjected to noise reduction using the signal space separation method with a temporal extension (correlation limit: 0.950; correlation window duration: 6 s).[69] Only data from the gradiometers were used for further analysis. For details regarding head surface
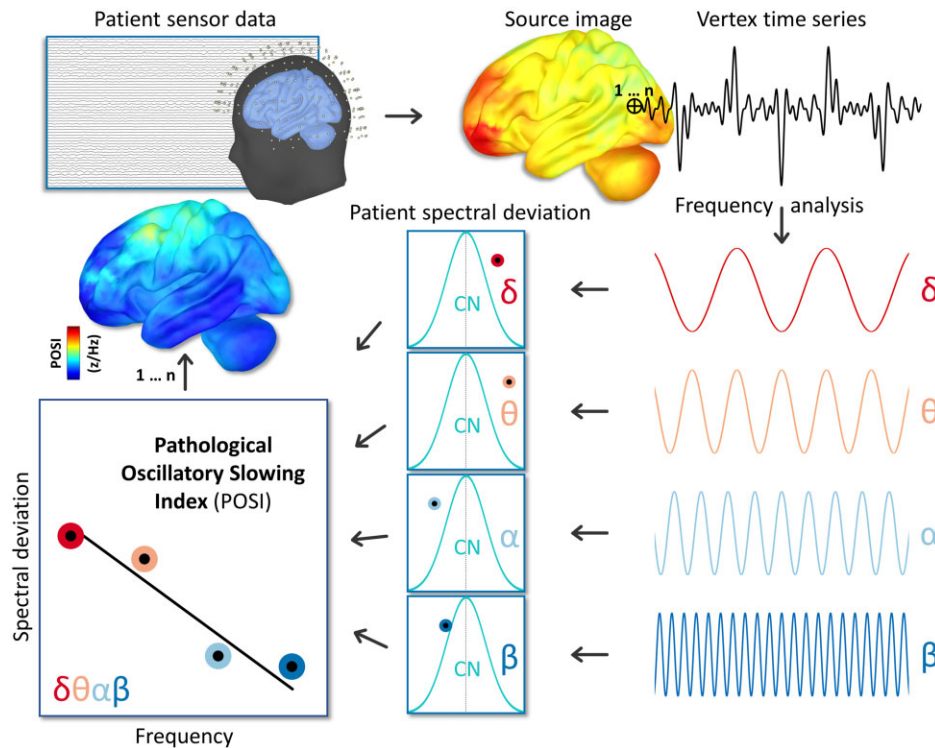
Figure 1 Computation of the POSI. Sensor-level data were imaged to the cortical surface for all participants (*top*) and these spatially resolved maps were decomposed into canonical frequency bands of interest per each vertex (*bottom right*). For each patient, these vertex-wise estimates of spectral neuronal amplitude were normalized to the distribution of comparable data (i.e. from the same vertex and frequency band) from the cognitively normal group to generate spatially resolved maps of pathological spectral deviation (*bottom middle*). A linear model was estimated for these patient spectral deviation scores as a function of frequency, and the slope of best fit was then extracted (*bottom left*) that represented the magnitude of neuronal oscillatory slowing relative to the cognitively normal control group. Such a model was estimated per each vertex, which resulted in a spatially resolved map of pathological oscillatory slowing for every patient.

digitization, coregistration, continuous head localization and pre-processing, see the Supplementary material.

Each participant's MEG data were co-registered with their own high-resolution structural T_1-weighted MRI data (Siemens Prisma 3 T; 64-channel head coil; repetition time: 2.3 s; echo time: 2.98 ms; flip angle: 9°; field of view: 256 mm; slice thickness: 1 mm; voxel size: 1 mm³) using an iterative closest-point rigid-body registration in *Brainstorm* (09/03/2020 distribution)[70] and, when necessary, these fits were manually corrected following visual inspection. Triangulated cortical surfaces were computed from the T_1 MRI data using FreeSurfer recon_all[71] using default settings and imported into *Brainstorm*. Individual cortical surfaces were down-sampled to 15 000 vertices (17 000 vertices including the cerebellum) for use in MEG source imaging.

MEG analysis

After preprocessing, the MEG data were source-imaged using an overlapping-spheres forward model, with source orientations unconstrained to the cortical surface. This approach spatially aligns the edge of each sphere nearest to its associated sensor with a dilated version of the cortical envelope (meant to approximate the inner surface of the skull) and has been found to produce comparable results to more computationally expensive boundary element method approaches.[72,73] A linearly constrained minimum variance beamformer implemented in *Brainstorm* was used to spatially filter the epoch-wise data based on the data covariance computed from the resting-state recording. These source-level time-series data were then transformed into the frequency-domain using Welch's method for estimating power spectral density (window = 1 s; 50%

overlap), grouped into canonical frequency bands (delta: 2–4 Hz; theta: 5–7 Hz; alpha: 8–12 Hz; beta: 15–29 Hz) and these frequency-wise maps were normalized to the total power across the frequency spectrum. The norm of the three unconstrained orientations of each of these maps was then projected onto a common FSAverage template surface (including the cerebellum) for statistical comparisons across participants.

These template-space neural MEG maps were used to compute a new frequency-normalized slope metric of pathological slowing per each participant and vertex, termed the POSI (Fig. 1). The first step of this computation was to compute the frequency-wise patient spectral deviation (PSD) per each Alzheimer's disease spectrum patient (i) and vertex (v):

$$PSD(i, v) = \frac{A(i, v) - \mu(v)_{CN}}{\sigma(v)_{CN}} \tag{1}$$

This step served to normalize the vertex-wise neural data within each of the four frequency bands (i.e. delta, theta, alpha and beta) per patient to the distribution of the cognitively normal group. From these normalized maps, we then fit a linear model across the four frequencies per participant and vertex using the *polyfit* function in MATLAB and extracted the estimated slope. These slopes represented the multi-frequency oscillatory slowing of neural activity for each patient, relative to the cognitively normal group, and importantly, retained the native resolution of our original source images. For interpretation, vertices with more negative slope values would indicate a stronger oscillatory slowing effect. Hypothesis-driven statistical comparisons were then computed using these spatially resolved POSI maps.

Statistical analysis and visualization

Statistical comparisons were performed, covarying out the effect of age, using SPM12. Initial tests using parametric general linear models were performed to investigate significant effects of spatially resolved pathological oscillatory slowing (i.e. one-sample test versus zero), effects of clinical determination on neural slowing (i.e. unpaired t-test between aMCI and probable Alzheimer's disease) and relationships between this spatially resolved slowing and cognitive function (i.e. regression of MoCA scores on POSI maps). To account for non-uniform spatial autocorrelation in the data, avoid the assumptions of parametric modelling and avoid selecting arbitrary cluster-forming thresholds, threshold-free cluster enhancement (TFCE; E = 1.0, H = 2.0; 5000 permutations)[74] was performed, with multiple comparisons correction set to cluster-wise $P_{FWE} < 0.05$. TFCE clusters surviving at this threshold were then used to create logical masks that were applied to the original statistical contrasts (i.e. vertex-wise F-values) for visualization in *Brainstorm*. Peak-vertex data from these clusters were extracted and plotted using *ggplot2*[75] for interpretation of directional effects. All region labels for interpretation of peak-vertex locations were derived from the Desikan–Killiany atlas.[76] In order to examine the relative contribution of each frequency band to the interparticipant variability of the POSI metric, band-limited power estimates were correlated with POSI values at each vertex using Pearson's r and plotted on surface maps for visualization.

The peak-vertex data from the POSI–MoCA relationship were also used to investigate the specific cognitive domains contributing to this effect, by computing *post hoc* regression models between POSI values at this peak and each domain-specific cognitive function in R.[77] To determine whether relationships between general cognitive function and POSI values were attributable to domain-specific cognitive impairments, causal mediation analysis with non-parametric bootstrapping (10 000 simulations) was conducted in R using the *mediation* package.[78] In addition to this more sensitive peak-vertex analysis (i.e. due to the smaller number of multiple comparisons to correct), we also regressed the POSI maps on scores from each individual cognitive domain, beyond the effects of age. Multiple comparisons correction for these tests used TFCE and a final threshold of $P_{FWE} < 0.01$ ($P_{FWE} < 0.05$, Bonferroni-corrected for the five cognitive domains).

To explore the potential clinical relevance of differing spatial patterns of neural slowing, we performed k-means clustering of the spatial POSI data. Details of this analysis can be found in the Supplementary material.

Linear mixed-effects modelling to test for relationships between regional amyloid-β uptake and POSI values was performed using the *nlme* package in R, with the following form: *POSI ~ SUVR + Age, random = (~1 | Patient/Vertex)*. To test the importance of this amyloid-β–POSI relationship for neuropsychological performance, Pearson correlations were computed for each patient between vertex-wise POSI and standardized uptake value ratio (SUVR) data then normalized using the Fisher transform. These normalized coefficients were then related to performance on the three neuropsychological domains that were previously found to covary with POSI (i.e. attention, verbal function and processing speed), above and beyond the effects of age, using multiple regression (Amyloid-β × POSI ~ Attention + Verbal + Processing Speed + Age; *lm* function in R).

The utility of the POSI for predicting Alzheimer's disease pathology beyond that of more straightforward spectral power derivations was tested using two approaches. First, we performed a vertex-wise model comparison of the previously mentioned POSI–MoCA regression and a comparable linear model of band-limited power in all four relevant frequencies (i.e. delta, theta, alpha and beta), and calculated differences in the Akaike information criterion (ΔAIC; absolute values

> 3 considered meaningful). Second, we performed model comparisons between the previously mentioned POSI–amyloid-β linear mixed-effects model and similar models for each of the four spectral frequencies, again using ΔAIC as our outcome metric.

Potential effects of clinical determination were examined by adding group (i.e. aMCI versus probable Alzheimer's disease) as an interacting factor in previously described statistical models, including the vertex-wise POSI–MoCA regression, the peak-vertex regressions of the POSI on domain-specific cognitive functions and the linear mixed effects models of the amyloid-β–POSI relationship.

To test the relative contribution of established functionally defined cortical networks[80] to the POSI–SUVR relationship, we included a new covariate in the previous linear mixed-effects model, with the following form: *POSI ~ SUVR + Age, random = (~1 | Patient/Network/Vertex)*. For each of the seven networks in the Yeo atlas (i.e. visual, dorsal attention, ventral attention, somato-motor, limbic, default mode and fronto-parietal), we computed this model without the vertices from the respective network and compared this 'missing-region' model to 100 models with an equivalent number of missing vertices from locations outside of that network. This resulted in 100 model comparison statistics (in ΔAIC) per network, representing the contribution of that region to the POSI–SUVR model, relative to equivalently sized random subsamples of the rest of the cortical surface.

Data availability

The data that support the findings of this study are available from the corresponding author, Dr Alex I. Wiesman, upon reasonable request.

Results

Aligning with previous research, grand averages of the spectrally and spatially resolved neural MEG maps revealed a subjective pattern of increased amplitude in lower frequencies and decreased amplitude in higher frequencies in patients on the Alzheimer's disease spectrum, as compared to the cognitively normal adults (Supplementary Fig. 1). These same MEG maps were used to compute spectral deviation maps for each patient on the Alzheimer's disease spectrum per canonical frequency band (Supplementary Fig. 2).

Evidence for spatially overlapping pathological oscillatory slowing in patients on the Alzheimer's disease spectrum

To determine which, if any, cortical regions exhibited a significant oscillatory neuronal slowing effect in patients on the Alzheimer's disease spectrum, we computed the novel spatially resolved POSI metric (Fig. 1; see the 'MEG analysis' section). Subjectively, this index indicated slowing across every lobe of the brain in the patients on the Alzheimer's disease spectrum; however, the magnitude of this effect varied substantially across the cortex (Supplementary Fig. 3). Statistical analysis indicated a robust effect in these patients across a distributed network encompassing the bilateral middle temporal (MTC), inferior parietal (IPC), medial temporal, dorsolateral prefrontal and cerebellar cortices (Fig. 2; see also Supplementary Fig. 4 for enhanced interpretation of this effect on the ventral cortical surface). The strongest evidence for this effect was found in the left (x, y, z: –64, –46, –7; $P_{FWE} < 0.001$) and right (48, –57, 9; $P_{FWE} = 0.001$) MTC and the left (–38, –67, –24; $P_{FWE} = 0.003$) and right (34, –50, –25; $P_{FWE} = 0.005$) cerebellum. In all of these regions, the direction of this significant slope was such
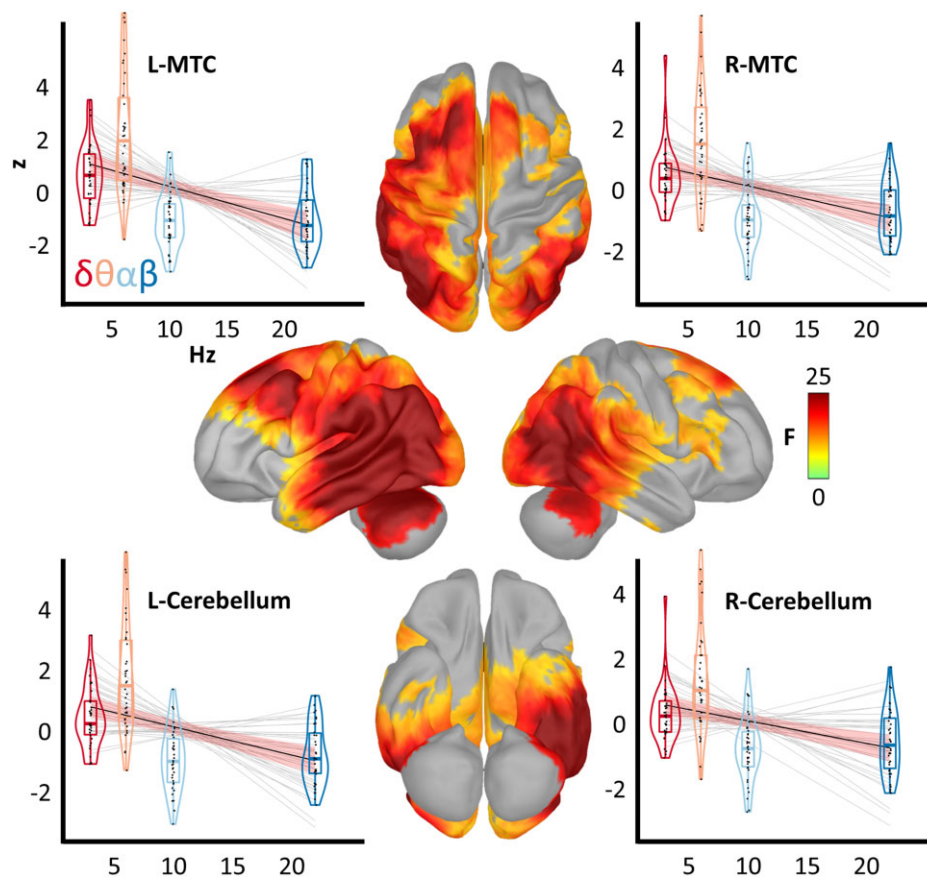
Figure 2 Regions of significant pathological oscillatory slowing in patients on the Alzheimer's disease spectrum. Surface maps indicate the results of a one sample test, controlling for age, of the vertex-wise POSI data against a null hypothesis of no significant slowing effect (i.e. an average slope of zero). The colour scale bar on the right indicates the statistical (F) values of this test. Importantly, only vertices exhibiting a significant slowing effect ($P_{FWE} < 0.05$) are shown in colour. Plots surrounding the surface maps represent the POSI relationships from the four vertices exhibiting the strongest slowing effects at the level of each patient, with frequency (in Hz) on the *x*-axis and patient spectral deviation (in *z*-scores) on the *y*-axis. Light grey lines represent lines of best fit from the linear model for each patient and the black line indicates the line of best fit across all patients, along with the corresponding model confidence intervals in salmon. For each frequency band of interest, box plots represent conditional means, first and third quartiles, and minima and maxima, and violin plots show the probability density. L/R = left/right.

that the amplitude of neuronal activity decreased as a function of frequency, providing robust support for a significant pathological oscillatory slowing effect in spatially overlapping neuronal populations in patients on the Alzheimer's disease spectrum. Correlation of the POSI values with band-limited estimates of neural amplitude indicated that all four frequencies (i.e. delta, theta, alpha and beta) contributed to the interparticipant variability of this metric, with beta and theta activity predicting the POSI most robustly (Supplementary Fig. 5).

Spatially resolved pathological oscillatory slowing predicts general and domain-specific cognitive function in patients on the Alzheimer's disease spectrum

Next, we investigated the relevance of this neural slowing effect to cognitive impairment among patients on the Alzheimer's disease spectrum. To test whether any spatial patterns of pathological oscillatory slowing related to general cognitive status, we first regressed each patient's MoCA scores on the vertex-wise POSI data. This revealed a significant relationship in a left lateralized cluster encompassing the middle and superior temporal cortex (STC), IPC and supramarginal (SMG) cortices (Fig. 3), with the most robust evidence for such an effect in the left STC (−52, 15, −22; $P_{FWE} = 0.024$) and SMG/

IPC (−38, −46, 39; $P_{FWE} = 0.032$). In all cases, the nature of this relationship was such that greater slowing of oscillatory neuronal activity predicted poorer cognitive function (peak $r_{partial} = 0.42$). No evidence for a significant effect of clinical determination (i.e. aMCI versus probable Alzheimer's disease) on this POSI–MoCA relationship was found (all vertex-wise P's > 0.05, uncorrected). Additionally, a model comparison approach indicated that the POSI was a better predictor of MoCA scores than simple spectral power derivatives across the vast majority of brain regions (Supplementary Fig. 6).

We then aimed to determine which cognitive domains might account for the association of general cognitive status with pathological oscillatory slowing. Towards this goal, we extracted POSI scores from the vertex exhibiting the strongest relationship with MoCA scores (left STC) and regressed these data on neuropsychological composite scores representing five cognitive domains (i.e. memory, learning, attention, verbal function and processing speed) known to be impacted in patients on the Alzheimer's disease spectrum. Importantly, all five cognitive domains were significantly correlated with MoCA scores (learning: $r = 0.71$; verbal function: $r = 0.83$; memory: $r = 0.35$; processing speed: $r = 0.69$; attention: $r = 0.71$; all P-values < 0.05), and so this approach was not disproportionately biased towards any single cognitive domain. Pathological slowing significantly predicted attention ($r_{partial} = 0.44$; $P = 0.006$), processing speed ($r_{partial} = 0.36$; $P = 0.028$) and verbal function ($r_{partial} = 0.34$; $P = 0.039$), indicating that the
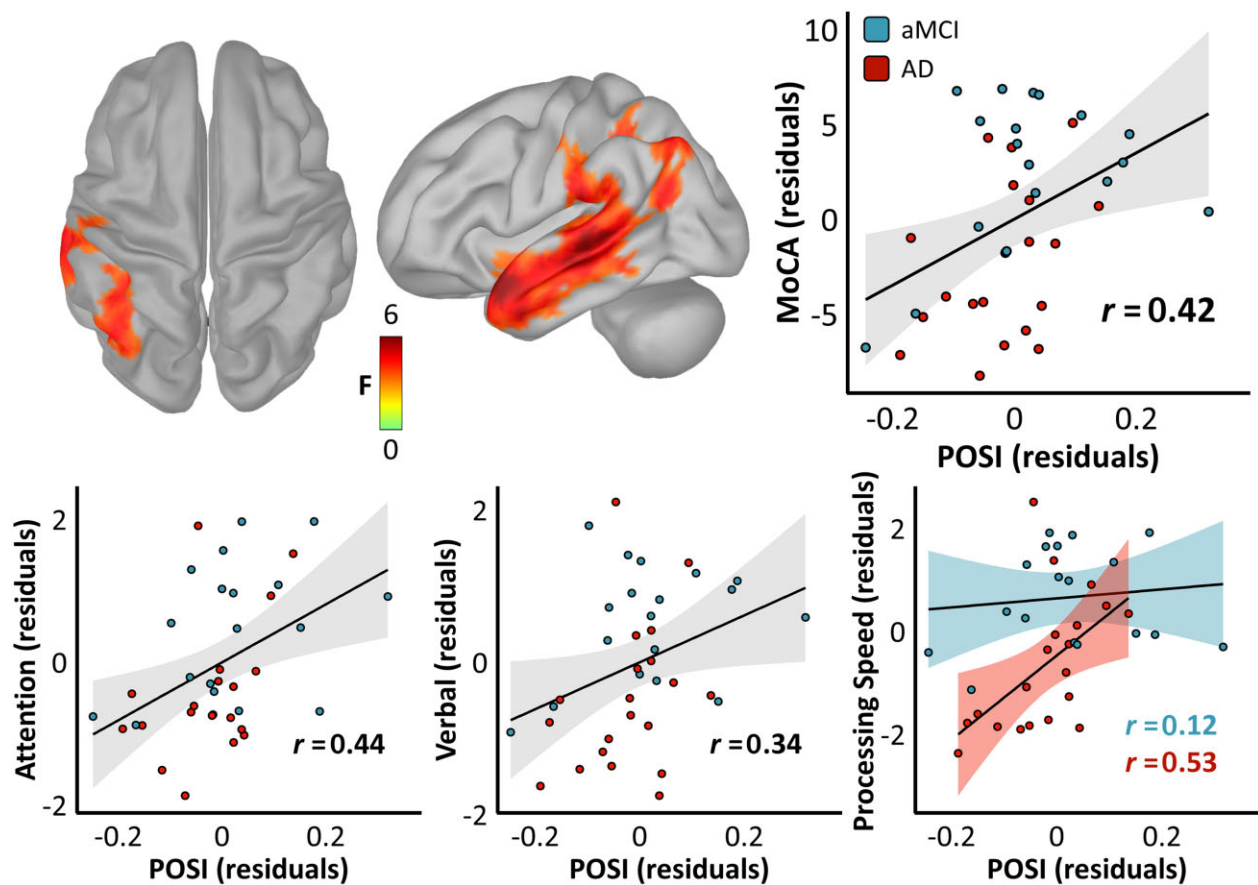
Figure 3 Relationships between pathological oscillatory neuronal slowing and cognitive function in patients on the Alzheimer's disease spectrum. Surface maps indicate the results of a regression of the vertex-wise POSI data against general cognitive function, as measured by the MoCA. The colour scale bar below the maps indicates the statistical (F) values of this test. Importantly, only vertices exhibiting a significant relationship between POSI and MoCA scores ($P_{FWE} < 0.05$) are shown in colour. The scatterplot to the *right* of the surface maps represents the POSI–MoCA relationship from the vertex exhibiting the strongest such effect (left STC; −52, 15, −22), with POSI residuals (in z/Hz) on the *x*-axis and MoCA residuals (in test units) on the *y*-axis. Clinical determination of each patient is indicated by the colour of each data-point [aMCI = blue, probable Alzheimer's disease (AD) = red]. The line of best fit for this relationship is overlaid in black, along with the corresponding confidence intervals in grey. Scatterplots below indicate similar relationships using POSI data from the same peak vertex for predicting domain-specific cognitive function, with the *y*-axes representing attention residuals on the *left*, verbal function residuals in the middle and processing speed residuals on the right (all in z-score units). Note that separate fit lines, confidence intervals and partial correlation coefficients are overlaid for each Alzheimer's disease spectrum subgroup for the relationship between the POSI and processing speed (*bottom right*), as a significant interaction effect of clinical determination on this relationship was present (no such interaction was observed for attention or verbal function).

relationship between pathological oscillatory slowing and cognitive declines in the Alzheimer's disease spectrum group is primarily due to deficits in these domains, rather than memory ($P = 0.352$) or learning ($P = 0.567$). Supporting this dissociation, *post hoc* Bayesian testing of the non-significant relationships between POSI values and learning ($BF_{01} = 2.24$) and memory ($BF_{01} = 1.73$) indicated evidence for the null hypothesis. Mediation testing using the weighted average of the attention, processing speed and verbal cognition scores revealed that the POSI–MoCA relationship was fully mediated by impairments in these domains [$\Delta R^2 = 0.493$, $P < 0.001$; indirect effect, average causal mediation effect = 14.10, $P = 0.001$; average direct effect = 3.57, $P = 0.488$]. Interestingly, the relationship between neural slowing and processing speed at this location was moderated by clinical determination, such that patients with probable Alzheimer's disease exhibited a significantly stronger pathological relationship ($r_{partial} = 0.53$) than those with aMCI [$r_{partial} = 0.12$; Fig. 3, bottom right; $t(33) = 2.41$, $P = 0.022$]. No other cognitive domains exhibited a significant interaction effect of clinical determination.

Spatially unrestricted (but more statistically conservative) tests for relationships between the POSI and cognitive domain scores

across all vertices also indicated a robust and widespread effect of neural slowing on processing speed, which spanned the IPC and MTC bilaterally (Supplementary Fig. 7; peak: left IPC, −41, −65, 33; $P_{FWE} = 0.006$; peak $r_{partial} = 0.40$). No other cognitive domains exhibited a significant relationship to neural slowing using this approach after corrections for multiple comparisons.

The spatial patterning of this slowing effect also provided meaningful information regarding domain-specific cognitive impairments. Spatial clustering identified five relatively distinct spatial 'subtypes' of neural slowing in our patient group, and the attentional abilities of participants varied significantly across these subtypes [$F(4,32) = 4.80$, $P = 0.004$; Supplementary Fig. 8]. These spatial patterns did not significantly predict differences in the other four domains.

Spatially resolved oscillatory slowing predicts the severity of regional amyloid-β burden

We next examined whether the severity of this spatially resolved pathological neural slowing effect covaried with the magnitude of regional amyloid-β burden, by computing a nested linear mixed-

effects model that incorporated shared spatial variability between these metrics at the level of each patient. The relationship between neural slowing and amyloid-β burden was highly significant [$t(570037) = -61.97$, $P < 0.001$], such that greater regional amyloid-β burden was associated with stronger oscillatory slowing across cortical regions, and this effect was greater in patients with probable Alzheimer's disease than those with aMCI [$t(570036) = -9.52$, $P < 0.001$; Fig. 4]. The POSI was also a better predictor of regional amyloid-β burden than simple spectral power derivatives in all four frequency-bands (i.e. delta, theta, alpha and beta; Supplementary Table 2).

The strength of the relationship between amyloid-β burden and neural slowing also predicted domain-specific cognitive abilities, such that patients with a stronger pathological (i.e. more negative) relationship between these two metrics exhibited worsened attention impairments ($r_{partial} = 0.45$; $P = 0.007$). Finally, by parcellating the MEG and PET data using an established atlas of human functional networks[80] and probing the relative importance of each of these networks to the neural slowing–amyloid-β relationship using a modified leave-one-out model comparison approach, we found that visual, limbic, dorsal attention and somatomotor networks contributed to this effect more substantially than ventral attention, fronto-parietal and default mode regions (Supplementary Fig. 9).

Discussion

Despite decades of research, direct support for an oscillatory slowing effect in spatially overlapping neuronal populations in patients on the Alzheimer's disease spectrum has been lacking. Further, a singular continuous metric of oscillatory neuronal slowing has not been developed, making it difficult to interpret whether such a slowing effect is in fact pathological in nature (i.e. as evidenced by relationships with cognitive decline and amyloid-β and/or tau burden). Using extensive neuropsychological testing, quantitative amyloid-PET and a novel continuous metric of spatially resolved oscillatory slowing based on MEG, we find evidence for a robust oscillatory neuronal slowing effect in a bilateral network of middle and medial temporal, IPC, dorsolateral prefrontal and cerebellar cortices in patients on the Alzheimer's disease spectrum.

Oscillatory slowing in left-lateralized MTC, SMG and IPC of these patients significantly predicted poorer general cognitive status (i.e. MoCA scores). *Post hoc* testing of these POSI data against cognitive domain scores indicated that the relationship between oscillatory slowing and cognitive decline was due to specific effects on attention, verbal function and processing speed and not the hallmark neuropsychological deficits of Alzheimer's disease (i.e. learning and memory). This indicates that, at least in the later stages of the Alzheimer's disease spectrum, neural slowing is a better indicator of executive and attentional impairments, rather than amnestic ones. It should be noted, however, that relationships between neural slowing and memory are still possible, or perhaps even likely, in the earlier preclinical or prodromal stages of the disease when amnestic impairments are beginning to emerge and are more variable across individuals. Further, spatial variations in this oscillatory slowing over the cortex were strongly related to the intensity of regional amyloid-β uptake, and the strength of this relationship predicted attention function, indicating a link to proteinopathy and providing additional evidence that this is a pathological effect. In some cases (e.g. POSI relationships with processing speed and amyloid-β), these pathological effects were stronger in patients with clinical determinations of probable Alzheimer's disease than those with aMCI, indicating a clinical progression of these effects along the Alzheimer's disease spectrum. These findings not only advance our understanding of

functional neuronal pathology in Alzheimer's disease, but also serve to validate a new measure of pathological oscillatory slowing that can be applied to a diverse range of patient populations.

Our finding of a spatially resolved oscillatory slowing effect in distinct regions of the temporal, parietal and prefrontal cortices in patients on the Alzheimer's disease spectrum provides strong evidence that the classical effect of increased low-frequency and decreased high-frequency activity in these patients does in fact represent a slowing of neuronal activity in spatially overlapping cell populations. While the spatial resolution of modern non-invasive neuroimaging limits our ability to conclude that this is necessarily occurring at the single cell or columnar level, it can now be said that such an effect is observed with the same neuronal population on the scale of local processing (e.g. at the level of individual gyri and sulci). By weighting our slowing metric both spatially and spectrally to comparable neuronal activity in a biomarker-negative group of cognitively normal older adults, we also show that this effect is not biased by natural frequency-wise differences in oscillatory amplitude. Additionally, as the weighted POSI scores retain this slowing information at the level of each patient, we are also able to use these whole-brain slowing maps to provide evidence for the pathological nature of this effect. Specifically, we found that oscillatory slowing in the temporal and parietal cortices predicted worse attention, processing speed and verbal function, as well as a measure of global cognitive function (i.e. MoCA scores) in patients on the Alzheimer's disease spectrum. A spatial clustering analysis also uncovered five relatively distinct spatial 'subtypes' of neural slowing in our sample and indicated that participants with different slowing subtypes exhibited systematic differences in attentional abilities. This finding is preliminary due to our limited sample size, but might indicate a valuable future direction for this work in using the POSI to differentiate disease subtypes in patients on the Alzheimer's disease spectrum.

This slowing effect also related robustly to a hallmark feature of Alzheimer's disease: regional accumulation of amyloid-β plaques, and the strength of this pathological relationship predicted attentional abilities. This provides additional evidence for the pathological nature of spatially resolved oscillatory slowing in Alzheimer's disease and indicates a potentially exciting new line of research into the epidemiological timeline and mechanisms of this relationship. A limited literature has explored the relationships between band-limited neural activity and proteinopathy in patients with Alzheimer's disease. In a small sample of amyloid-β-positive patients with Alzheimer's disease ($n = 7$), Coomans *et al.*[36] found a bidirectional relationship between spectral neural power and tau pathology, such that greater regional tau deposition predicted increased delta activity but decreased theta and alpha activity. This suggested a potential relationship between Alzheimer's disease proteinopathy and a generalized slowing of neural activity, which our findings confirm, albeit with amyloid-β pathology rather than tau. Another study by Ranasinghe *et al.*[34] related band-limited neural synchrony (i.e. the statistical similarity of neural activity between regions) to regional amyloid-β and tau pathology, and found that hypersynchronous neural activity in the delta and theta range in patients with Alzheimer's disease colocalized with both tau and amyloid-β, whereas hyposynchrony in the alpha band colocalized only with tau. Additional work confirmed the alpha–tau relationship post-mortem.[35] Although they did not test for such an effect statistically, these studies suggested a potential relationship between Alzheimer's disease proteinopathy and slowing of neural connectivity, indicating that the effects we report herein might propagate to interregional neural communication. Thus, computing our novel metric of neural slowing on band-limited functional connectivity data and then relating this to Alzheimer's disease proteinopathy would be a valuable next
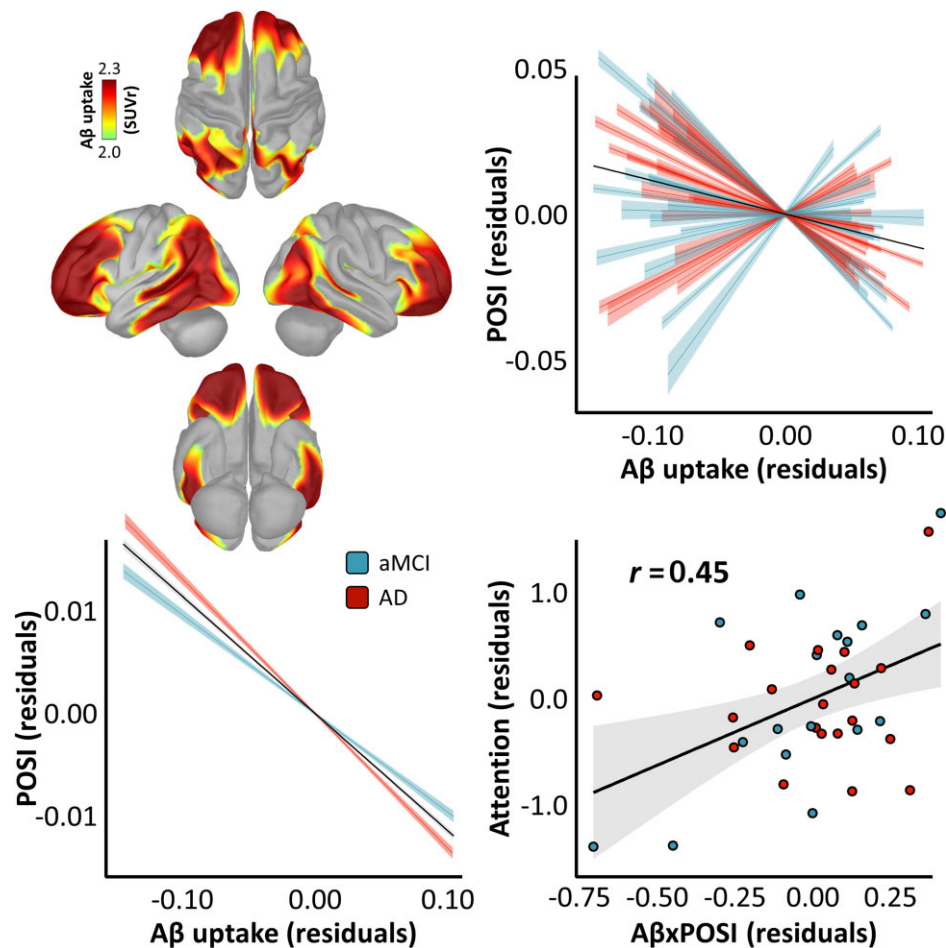
Figure 4 Relationships between pathological oscillatory neuronal slowing, regional amyloid-β uptake and cognition in patients on the Alzheimer's disease spectrum. Surface maps on the *top left* indicate the mean vertex-wise uptake of amyloid-β (Aβ), measured by quantitative ^{18}F florbetapir PET, in SUVRs. The spatial correspondence between this regional amyloid-β uptake and the pathological oscillatory slowing effect is indicated by the plot on the *top right*, where the individual model fit (with corresponding confidence intervals) between these measures over all cortical vertices is indicated for each patient by the coloured fit lines and the overall model fit (again with confidence intervals) is overlaid in black. The comparable plot on the *bottom left* indicates the significant interaction effect of clinical determination on the POSI–amyloid-β relationship. The plot on the *bottom right* indicates the impact of the magnitude of this pathological relationship (*x*-axis) on attentional abilities (*y*-axis), with the partial correlation coefficient, line-of-best-fit and corresponding confidence intervals overlaid. Note that more negative values on the *x*-axis indicate a stronger pathological relationship between regional amyloid-β burden and neural slowing. For all plots, clinical determination is indicated by the colour of each data-point/fit line (aMCI = blue, probable Alzheimer's disease = red).

direction for this work. It should also be noted that these studies all leveraged the substantial variability of PET and MEG metrics across cortical regions, rather than across participants, for statistical modelling. In contrast, Nakamura *et al.*[37] tested for differences in spectral neural power between participants with and without amyloid-β positivity who were either asymptomatic or in the prodromal stages of the disease. In contrast to our findings, they found that amyloid-β-positive participants exhibited stronger alpha activity in prefrontal cortices compared to those who were amyloid-β-negative. However, this discrepancy is very likely due to differences in patient populations, as our group was at a more advanced stage of the disease. Future research investigating neural slowing in participants who are healthy and/or in the preclinical stages of Alzheimer's disease would thus be useful to resolve this.

Our observed relationship between amyloid-β burden and neural slowing in these patients implies a relative shift towards macro-scale hypoexcitability in brain regions with higher amyloid-β accumulation. Previous work has found a hyperexcitable effect of amyloid-β on neural activity in the preclinical-to-prodromal stages of the disease in humans[33,37,81] and in non-human animal

and *in vitro* Alzheimer's disease models that do not fully recapitulate the late-stage disease process.[82–89] This effect shifts towards hypoexcitability at later stages of Alzheimer's disease,[33,90–92] signifying synapse failure and neurodegeneration. Given that patients were required to exhibit clinically significant cognitive impairments for inclusion in our study, our findings provide further support for a shift towards a hypoexcitable effect of amyloid-β on neural activity in the later stages of Alzheimer's disease, represented here as a macro-level shift towards activity in slower frequencies. The logical next step in this line of research is to model this neural slowing–amyloid-β relationship in a cohort of cognitively normal older adults, with the expectation that regional amyloid-β burden would instead predict a relative *acceleration* of neural activity in the preclinical/asymptomatic stages of Alzheimer's disease pathology.

While exciting, these findings are not without limitations. First, the spatial resolution of MEG in detecting neural sources farther away from the sensors is relatively low, particularly for data recorded from gradiometers. Although the robust oscillatory slowing effect that we observed extended into parahippocampal

cortices bilaterally, we are unable to make strong claims here about whether such a slowing effect exists in the hippocampus proper, as might be expected. Targeted studies using data recorded from magnetometers (i.e. rather than gradiometers) and/or recent advances in MEG sensor technology,[93] coupled with discrete models of medial temporal cortex structures, might better address this question. Second, although we made efforts to include as wide a range of patients on the Alzheimer's disease spectrum as possible, our inclusion requirement of clinically significant cognitive impairments likely limited our sample to relatively late stages of the disease. As mentioned above, expanding our sample size and extending study recruitment to earlier preclinical and/or prodromal participant groups will provide key insights into the non-linear effects of amyloid-β on neural function across the Alzheimer's disease spectrum, and might also reveal additional, more variable/sensitive relationships between neural slowing and cognition. A more detailed assessment of the relationships between spatial subtypes of neural slowing and variations in clinical presentation would also be possible with a larger and more heterogeneous patient sample, and might enhance our understanding of the neural bases of less-common Alzheimer's disease variants (e.g. posterior cortical atrophy, logopenic variant primary progressive aphasia and behavioural/dysexecutive predominant subtypes). Third, while our novel neural slowing metric did relate to many clinical and pathological hallmarks of Alzheimer's disease in this study, it is clear that additional research regarding its specificity and sensitivity are required. If these studies indicate a strong clinical potential for this metric, then this approach to modelling multi-spectral functional neural pathology as a single continuous metric at the level of individual patients might lend itself exceedingly well to a clinical setting, similar to the current approach of reading normalized PET scans by neurologists or radiologists.

Before closing, the potential utility of the POSI for future research and clinical use should also be noted. The POSI represents a robust multi-spectral derivative of simple MEG resting-state recordings and can be computed at the level of individual patients, making it an ideal candidate for the tracking of functional neural changes and clinical progression. Further, we found this metric to be a better predictor of both general cognitive function and regional amyloid-β burden than simple spectral power derivatives, signifying the potential value of this approach. Although we conceptualize and validate this metric in patients on the Alzheimer's disease spectrum, a number of other neurological and psychiatric disorders have been characterized by similar neuronal slowing patterns. Most notably, patients with Parkinson's disease have exhibited a robust slowing effect in previous MEG/EEG studies[94–97] that track cognitive decline longitudinally.[98] Children born very preterm have also shown similar neuronal changes,[99] as have individuals with neuropathic pain.[100,101] However, these studies suffer from similar shortcomings regarding spatial specificity and links to clinical outcomes. Using the POSI, a much clearer, more spatially resolved understanding of these neuronal pathologies is possible, with hopes of progressing these lines of research towards clinical intervention and early detection.

Acknowledgements

Funding

Competing interests

The authors declare no competing conflicts of interest, financial or otherwise.

Supplementary material

Supplementary material is available at *Brain* online.

References

1. Jones DT, Knopman DS, Gunter JL, et al.; Alzheimer's Disease Neuroimaging Initiative. Cascading network failure across the Alzheimer's disease spectrum. *Brain*. 2016;139(Pt 2):547–562.
2. Jack CR Jr, Wiste HJ, Weigand SD, et al. Defining imaging biomarker cut points for brain aging and Alzheimer's disease. *Alzheimer's Dement*. 2017;13(3):205–216.
3. Aisen PS, Cummings J, Jack CR, et al. On the path to 2025: Understanding the Alzheimer's disease continuum. *Alzheimer's Res Ther*. 2017;9(1):60.
4. Ewers M, Walsh C, Trojanowski JQ, et al.; North American Alzheimer's Disease Neuroimaging Initiative (ADNI). Prediction of conversion from mild cognitive impairment to Alzheimer's disease dementia based upon biomarkers and neuropsychological test performance. *Neurobiol Aging*. 2012;33(7):1203–1214.e2.
5. Ossenkoppele R, Smith R, Ohlsson T, et al. Associations between tau, Aβ, and cortical thickness with cognition in Alzheimer disease. *Neurology*. 2019;92(6):e601–e612.
6. Mattsson N, Insel PS, Donohue M, et al. Predicting diagnosis and cognition with 18F-AV-1451 tau PET and structural MRI in Alzheimer's disease. *Alzheimer's Dement*. 2019;15(4):570–580.
7. Pontecorvo MJ, Devous MD Sr, Navitsky M, et al.; 18F-AV-1451-A05 investigators. Relationships between flortaucipir PET tau binding and amyloid burden, clinical diagnosis, age and cognition. *Brain*. 2017;140(3):748–763.
8. Ossenkoppele R, Schonhaut DR, Schöll M, et al. Tau PET patterns mirror clinical and neuroanatomical variability in Alzheimer's disease. *Brain*. 2016;139(5):1551–1567.
9. Weiner MW, Veitch DP, Aisen PS, et al.; Alzheimer's Disease Neuroimaging Initiative. Recent publications from the Alzheimer's Disease neuroimaging initiative: Reviewing progress toward improved AD clinical trials. *Alzheimer's Dement*. 2017;13(4):e1–e85.
10. Hampel H, Bürger K, Teipel SJ, Bokde AL, Zetterberg H, Blennow K. Core candidate neurochemical and imaging biomarkers of Alzheimer's disease. *Alzheimer's Dement*. 2008;4(1):38–48.
11. O'brien J, O'keefe K, LaViolette P, et al. Longitudinal fMRI in elderly reveals loss of hippocampal activation with clinical decline. *Neurology*. 2010;74(24):1969–1976.

12. Wang K, Liang M, Wang L, et al. Altered functional connectivity in early Alzheimer's disease: A resting-state fMRI study. *Hum Brain Mapp*. 2007;28(10):967–978.

13. Greicius MD, Srivastava G, Reiss AL, Menon V. Default-mode network activity distinguishes Alzheimer's disease from healthy aging: Evidence from functional MRI. *Proc Natl Acad Sci*. 2004;101(13):4637–4642.

14. Agosta F, Pievani M, Geroldi C, Copetti M, Frisoni GB, Filippi M. Resting state fMRI in Alzheimer's disease: Beyond the default mode network. *Neurobiol Aging*. 2012;33(8):1564–1578.

15. Badhwar A, Tam A, Dansereau C, Orban P, Hoffstaedter F, Bellec P. Resting-state network dysfunction in Alzheimer's disease: A systematic review and meta-analysis. *Alzheimer's Dement*. 2017;8:73–85.

16. Osipova D, Ahveninen J, Jensen O, Ylikoski A, Pekkonen E. Altered generation of spontaneous oscillations in Alzheimer's disease. *Neuroimage*. 2005;27(4):835–841.

17. Engels M, van Der Flier W, Stam C, Hillebrand A, Scheltens P, van Straaten E. Alzheimer's disease: The state of the art in resting-state magnetoencephalography. *Clin Neurophysiol*. 2017;128(8):1426–1437.

18. Mandal PK, Banerjee A, Tripathi M, Sharma A. A comprehensive review of magnetoencephalography (MEG) studies for brain functionality in healthy aging and Alzheimer's disease (AD). *Front Comput Neurosci*. 2018;12:60.

19. Fernández A, Maestú F, Amo C, et al. Focal temporoparietal slow activity in Alzheimer's disease revealed by magnetoencephalography. *Biol Psychiatry*. 2002;52(7):764–770.

20. Penttilä M, Partanen JV, Soininen H, Riekkinen P. Quantitative analysis of occipital EEG in different stages of Alzheimer's disease. *Electroencephalogr Clin Neurophysiol*. 1985;60(1):1–6.

21. Schreiter-Gasser U, Gasser T, Ziegler P. Quantitative EEG analysis in early onset Alzheimer's disease: A controlled study. *Electroencephalogr Clin Neurophysiol*. 1993;86(1):15–22.

22. Huang C, Wahlund L-O, Dierks T, Julin P, Winblad B, Jelic V. Discrimination of Alzheimer's disease and mild cognitive impairment by equivalent EEG sources: A cross-sectional and longitudinal study. *Clin Neurophysiol*. 2000;111(11):1961–1967.

23. Başar E, Başar-Eroğlu C, Karakaş S, Schürmann M. Brain oscillations in perception and memory. *Int J Psychophysiol*. 2000;35(2-3):95–124.

24. Başar E, Başar-Eroglu C, Karakaş S, Schürmann M. Gamma, alpha, delta, and theta oscillations govern cognitive processes. *Int J Psychophysiol*. 2001;39(2-3):241–248.

25. Baillet S. Magnetoencephalography for brain electrophysiology and imaging. *Nat Neurosci*. 2017;20(3):327–339.

26. Ward LM. Synchronous neural oscillations and cognitive processes. *Trends Cogn Sci*. 2003;7(12):553–559.

27. Buzsaki G, Draguhn A. Neuronal oscillations in cortical networks. *Science*. 2004;304(5679):1926–1929.

28. Wiesman AI, O'Neill J, Mills MS, et al. Aberrant occipital dynamics differentiate HIV-infected patients with and without cognitive impairment. *Brain*. 2018;141(6):1678–1690.

29. Başar E, Güntekin B. Review of delta, theta, alpha, beta, and gamma response oscillations in neuropsychiatric disorders. *Suppl Clin Neurophysiol*. 2013;62:303–341.

30. Stam C. Use of magnetoencephalography (MEG) to study functional brain networks in neurodegenerative disorders. *J Neurol Sci*. 2010;289(1-2):128–134.

31. Wilson TW, Heinrichs-Graham E, Proskovec AL, McDermott TJ. Neuroimaging with magnetoencephalography: A dynamic view of brain pathophysiology. *Transl Res*. 2016;175:17–36.

32. Cuesta P, Barabash A, Aurtenetxe S, et al. Source analysis of spontaneous magnetoencephalograpic activity in healthy aging and mild cognitive impairment: Influence of apolipoprotein E polymorphism. *J Alzheimer's Dis*. 2015;43(1):259–273.

33. Koelewijn L, Lancaster TM, Linden D, et al. Oscillatory hyperactivity and hyperconnectivity in young APOE-ε4 carriers and hypoconnectivity in Alzheimer's disease. *Elife*. 2019;8:e36011.

34. Ranasinghe KG, Cha J, Iaccarino L, et al. Neurophysiological signatures in Alzheimer's disease are distinctly associated with TAU, amyloid-β accumulation, and cognitive decline. *Sci Transl Med*. 2020;12(534):eaaz4069.

35. Ranasinghe KG, Petersen C, Kudo K, et al. Reduced synchrony in alpha oscillations during life predicts post mortem neurofibrillary tangle density in early-onset and atypical Alzheimer's disease. *Alzheimer's Dement*. 2021.

36. Coomans EM, Schoonhoven DN, Tuncel H, et al. In vivo tau pathology is associated with synaptic loss and altered synaptic function. *Alzheimer's Res Ther*. 2021;13(1):35.

37. Nakamura A, Cuesta P, Fernández A, et al. Electromagnetic signatures of the preclinical and prodromal stages of Alzheimer's disease. *Brain*. 2018;141(5):1470–1485.

38. Dauwels J, Vialatte F, Cichocki A. Diagnosis of Alzheimer's disease from EEG signals: Where are we standing? *Curr Alzheimer Res*. 2010;7(6):487–505.

39. Dauwels J, Srinivasan K, Ramasubba Reddy M, et al. Slowing and loss of complexity in Alzheimer's EEG: Two sides of the same coin? *Int J Alzheimer's Dis*. 2011;2011:539621.

40. Dringenberg HC. Alzheimer's disease: More than a 'cholinergic disorder'—Evidence that cholinergic–monoaminergic interactions contribute to EEG slowing and dementia. *Behav Brain Res*. 2000;115(2):235–249.

41. Berendse H, Verbunt J, Scheltens P, Van Dijk B, Jonkman E. Magnetoencephalographic analysis of cortical activity in Alzheimer's disease: A pilot study. *Clin Neurophysiol*. 2000;111(4):604–612.

42. Fernández A, Hornero R, Mayo A, Poza J, Gil-Gregorio P, Ortiz T. MEG spectral profile in Alzheimer's disease and mild cognitive impairment. *Clin Neurophysiol*. 2006;117(2):306–314.

43. Montez T, Poil S-S, Jones BF, et al. Altered temporal correlations in parietal alpha and prefrontal theta oscillations in early-stage Alzheimer disease. *Proc Natl Acad Sci*. 2009;106(5):1614–1619.

44. de Haan W, Stam CJ, Jones BF, Zuiderwijk IM, van Dijk BW, Scheltens P. Resting-state oscillatory brain dynamics in Alzheimer disease. *J Clin Neurophysiol*. 2008;25(4):187–193.

45. Jafari Z, Kolb BE, Mohajerani MH. Neural oscillations and brain stimulation in Alzheimer's disease. *Progr Neurobiol*. 2020;194:101878.

46. Poza J, Hornero R, Abásolo D, Fernández A, Mayo A. Evaluation of spectral ratio measures from spontaneous MEG recordings in patients with Alzheimer's disease. *Comput Methods Prog Biomed*. 2008;90(2):137–147.

47. Soininen H, Reinikainen K, Partanen J, et al. Slowing of the dominant occipital rhythm in electroencephalogram is associated with low concentration of noradrenaline in the thalamus in patients with Alzheimer's disease. *Neurosci Lett*. 1992;137(1):5–8.

48. Garcés P, Vicente R, Wibral M, et al. Brain-wide slowing of spontaneous alpha rhythms in mild cognitive impairment. *Front Aging Neurosci*. 2013;5:100.

49. Engels M, Hillebrand A, van der Flier WM, Stam CJ, Scheltens P, van Straaten EC. Slowing of hippocampal activity correlates with cognitive decline in early onset Alzheimer's disease. An MEG study with virtual electrodes. *Front Hum Neurosci*. 2016;10:238.

50. Ostlund BD, Alperin BR, Drew T, Karalunas SL. Behavioral and cognitive correlates of the aperiodic (1/f-like) exponent of the EEG power spectrum in adolescents with and without ADHD. *Dev Cogn Neurosci*. 2021;48:100931.

51. Van Heumen S, Moreau JT, Simard-Tremblay E, Albrecht S, Dudley RW, Baillet SC. Report: Aperiodic fluctuations of neural activity in the Ictal MEG of a child with drug-resistant fronto-temporal epilepsy. *Front Hum Neurosci.* 2021;15:646426.

52. Pani SM, Fraschini M, Figorilli M, Tamburrino L, Ferri R, Puligheddu M. Sleep-related hypermotor epilepsy and non-rapid eye movement parasomnias: Differences in the periodic and aperiodic component of the electroencephalographic power spectra. *J Sleep Res.* 2021;30(5):e13339.

53. Wilkinson CL, Nelson CA. Increased aperiodic gamma power in young boys with Fragile X Syndrome is associated with better language ability. *Mol Autism.* 2021;12(1):1–15.

54. Peterson EJ, Rosen BQ, Campbell AM, Belger A, Voytek B. 1/f neural noise is a better predictor of schizophrenia than neural oscillations. *bioRxiv.* [Preprint] https://doi.org/10.1101/113449

55. McKhann GM, Knopman DS, Chertkow H, et al. The diagnosis of dementia due to Alzheimer's disease: Recommendations from the National Institute on Aging-Alzheimer's Association workgroups on diagnostic guidelines for Alzheimer's disease. *Alzheimer's Dement.* 2011;7(3):263–269.

56. Minoshima S, Drzezga AE, Barthel H, et al. SNMMI procedure standard/EANM practice guideline for amyloid PET imaging of the brain 1.0. *J Nucl Med.* 2016;57(8):1316–1322.

57. Wechsler D. *Advanced clinical solutions for the WAIS-IV and WMS-IV.* San Antonio, TX: The Psychological Corporation; 2009.

58. Heaton R, Miller SW, Taylor MJ, Grant I. *Revised comprehensive norms for an expanded Halstead-Reitan Battery: Demographically adjusted neuropsychological norms for African American and Caucasian adults.* Lutz, FL: Psychological Assessment Resources; 2004.

59. Wechsler D. *Wechsler adult intelligence scale–Fourth Edition (WAIS–IV).* San Antonio, TX: NCS Pearson; 2008;22(498):1.

60. Brandt J, Benedict RH. *Hopkins verbal learning test–revised: Professional manual.* Psychological Assessment Resources; 2001.

61. Nasreddine ZS, Phillips NA, Bédirian V, et al. The Montreal Cognitive Assessment, MoCA: A brief screening tool for mild cognitive impairment. *J Am Geriatr Soc.* 2005;53(4):695–699.

62. Folstein MF, Folstein SE, McHugh PR. "Mini-mental state": A practical method for grading the cognitive state of patients for the clinician. *J Psychiatr Res.* 1975;12(3):189–198.

63. Wiesman AI, Da Silva Castanheira J, Baillet S. Stability of spectral estimates in resting-state magnetoencephalography: Recommendations for minimal data duration with neuroanatomical specificity. *Neuroimage.* 2022;247:118823.

64. Pusil S, López ME, Cuesta P, Bruña R, Pereda E, Maestú F. Hypersynchronization in mild cognitive impairment: The 'X' model. *Brain.* 2019;142(12):3936–3950.

65. Ramírez-Toraño F, García-Alba J, Bruña R, et al. Hypersynchronized magnetoencephalography brain networks in patients with mild cognitive impairment and Alzheimer's disease in Down syndrome. *Brain Connect.* 2021;11(9):725–733.

66. de Haan W, van der Flier WM, Wang H, Van Mieghem PF, Scheltens P, Stam CJ. Disruption of functional brain networks in Alzheimer's disease: What can we learn from graph spectral analysis of resting-state magnetoencephalography? *Brain Connect.* 2012;2(2):45–55.

67. Stam C, De Haan W, Daffertshofer A, et al. Graph theoretical analysis of magnetoencephalographic functional connectivity in Alzheimer's disease. *Brain.* 2009;132(Pt 1):213–224.

68. Koelewijn L, Bompas A, Tales A, et al. Alzheimer's disease disrupts alpha and beta-band resting-state oscillatory network connectivity. *Clin Neurophysiol.* 2017;128(11):2347–2357.

69. Taulu S, Simola J. Spatiotemporal signal space separation method for rejecting nearby interference in MEG measurements. *Phys Med Biol.* 2006;51(7):1759–1768.

70. Tadel F, Baillet S, Mosher JC, Pantazis D, Leahy RM. Brainstorm: A user-friendly application for MEG/EEG analysis. *Comput Intell Neurosci.* 2011;2011:879716.

71. Fischl B. FreeSurfer. *Neuroimage.* 2012;62(2):774–781.

72. Huang M, Mosher JC, Leahy R. A sensor-weighted overlapping-sphere head model and exhaustive head model comparison for MEG. *Phys Med Biol.* 1999;44(2):423–440.

73. Henson R, Mattout J, Phillips C, Friston KJ. Selecting forward models for MEG source-reconstruction using model-evidence. *Neuroimage.* 2009;46(1):168–176.

74. Smith SM, Nichols TE. Threshold-free cluster enhancement: Addressing problems of smoothing, threshold dependence and localisation in cluster inference. *Neuroimage.* 2009;44(1):83–98.

75. Wickham H. *ggplot2: Elegant graphics for data analysis.* Springer; 2016.

76. Desikan RS, Ségonne F, Fischl B, et al. An automated labeling system for subdividing the human cerebral cortex on MRI scans into gyral based regions of interest. *Neuroimage.* 2006;31(3):968–980.

77. R Core Team. *R: A language and environment for statistical computing.* Vienna, Austria: R Foundation for Statistical Computing; 2017.

78. Tingley D, Yamamoto T, Hirose K, Keele L, Imai K. Mediation: R package for causal mediation analysis. *J Stat Softw.* 2014;59(5):

79. Kodinariya TM, Makwana PR. Review on determining number of cluster in k-means clustering. *Int J.* 2013;1(6):90–95.

80. Yeo BT, Krienen FM, Sepulcre J, et al. The organization of the human cerebral cortex estimated by intrinsic functional connectivity. *J Neurophysiol.* 2011;106(3):1125–1165.

81. Canuet L, Pusil S, López ME, et al. Network disruption and cerebrospinal fluid amyloid-beta and phospho-tau levels in mild cognitive impairment. *J Neurosci.* 2015;35(28):10325–10330.

82. Busche MA, Konnerth A. Impairments of neural circuit function in Alzheimer's disease. *Philos Trans R Soc B Biol Sci.* 2016;371(1700):20150429.

83. Busche MA, Konnerth A. Neuronal hyperactivity–A key defect in Alzheimer's disease? *Bioessays.* 2015;37(6):624–632.

84. Busche MA, Chen X, Henning HA, et al. Critical role of soluble amyloid-β for early hippocampal hyperactivity in a mouse model of Alzheimer's disease. *Proc Natl Acad Sci.* 2012;109(22):8740–8745.

85. Busche MA, Eichhoff G, Adelsberger H, et al. Clusters of hyperactive neurons near amyloid plaques in a mouse model of Alzheimer's disease. *Science.* 2008;321(5896):1686–1689.

86. Hector A, Brouillette J. Hyperactivity induced by soluble amyloid-β oligomers in the early stages of Alzheimer's disease. *Front Mol Neurosci.* 2020;13:600084.

87. Maestú F, de Haan W, Busche MA, DeFelipe J. Neuronal excitation/inhibition imbalance: A core element of a translational perspective on Alzheimer pathophysiology. *Ageing Res Rev.* 2021;69:101372.

88. Sosulina L, Mittag M, Geis HR, et al. Hippocampal hyperactivity in a rat model of Alzheimer's disease. *J Neurochem.* 2021;157(6):2128–2144.

89. Zott B, Simon MM, Hong W, et al. A vicious cycle of β amyloid-dependent neuronal hyperactivation. *Science.* 2019;365(6453):559–565.

90. Palop JJ, Mucke L. Amyloid-β-induced neuronal dysfunction in Alzheimer's disease: From synapses toward neural networks. *Nat Neurosci.* 2010;13(7):812–818.

91. Bass B, Upson S, Roy K, Montgomery EL, Jalonen TO, Murray IV. Glycogen and amyloid-beta: Key players in the shift from neuronal hyperactivity to hypoactivity observed in Alzheimer's disease? *Neural Regener Res.* 2015;10(7):1023–1025.

92. Stargardt A, Swaab DF, Bossers K. The storm before the quiet: Neuronal hyperactivity and Aβ in the presymptomatic stages of Alzheimer's disease. *Neurobiol Aging*. 2015;36(1): 1–11.

93. Boto E, Holmes N, Leggett J, et al. Moving magnetoencephalography towards real-world applications with a wearable system. *Nature*. 2018;555(7698):657–661.

94. Soikkeli R, Partanen J, Soininen H, Pääkkönen A, Riekkinen P Sr. Slowing of EEG in Parkinson's disease. *Electroencephalogr Clin Neurophysiol*. 1991;79(3):159–165.

95. Stoffers D, Bosboom J, Deijen J, Wolters EC, Berendse H, Stam C. Slowing of oscillatory brain activity is a stable characteristic of Parkinson's disease without dementia. *Brain*. 2007;130(Pt 7): 1847–1860.

96. Vardy AN, van Wegen EE, Kwakkel G, Berendse HW, Beek PJ, Daffertshofer A. Slowing of M1 activity in Parkinson's disease during rest and movement—An MEG study. *Clin Neurophysiol*. 2011;122(4):789–795.

97. Tanaka H, Koenig T, Pascual-Marqui RD, Hirata K, Kochi K, Lehmann D. Event-related potential and EEG measures in Parkinson's disease without and with dementia. *Dement Geriatr Cogn Disord*. 2000;11(1):39–45.

98. Olde Dubbelink KTE, Hillebrand A, Stoffers D, et al. Disrupted brain network topology in Parkinson's disease: A longitudinal magnetoencephalography study. *Brain*. 2014;137(Pt 1):197–207.

99. Doesburg SM, Ribary U, Herdman AT, et al. Magnetoencephalography reveals slowing of resting peak oscillatory frequency in children born very preterm. *Pediatr Res*. 2011;70(2):171–175.

100. Boord P, Siddall P, Tran Y, Herbert D, Middleton J, Craig A. Electroencephalographic slowing and reduced reactivity in neuropathic pain following spinal cord injury. *Spinal Cord*. 2008;46(2):118–123.

101. Sarnthein J, Stern J, Aufenberg C, Rousson V, Jeanmonod D. Increased EEG power and slowed dominant frequency in patients with neurogenic pain. *Brain*. 2006;129(Pt 1):55–64.